Scientific Reports

https://doi.org/10.1038/s41598-026-57733-6

Article in Press

Surface and elemental analysis of stainless-steel needles after invasive physiotherapy: an exploratory scanning electron microscopy (SEM) study

Received: 24 June 2024

Accepted: 9 June 2026

Published online: 15 July 2026

Cite this article as: Poveda-Pagán E.J., Lozano-Quijada C., Toledo-Marhuenda J.V. *et al.* Surface and elemental analysis of stainless-steel needles after invasive physiotherapy: an exploratory scanning electron microscopy (SEM) study. *Sci Rep* (2026). https://doi.org/10.1038/s41598-026-57733-6

Emilio J. Poveda-Pagán, Carlos Lozano-Quijada, José Vicente Toledo-Marhuenda, José Vicente Segura-Heras & Manel Santafé

Title: "**Surface and elemental analysis of stainless-steel needles after invasive physiotherapy: An exploratory scanning electron microscopy (SEM) study**"

Short Title: **Chemical analysis of needles used in humans**

Emilio J. Poveda-Pagán[1], Carlos Lozano-Quijada[1]*, José Vicente Toledo-Marhuenda[1], José Vicente Segura-Heras[2], Manel Santafé[3]

[1] Centro de Investigación Traslacional en Fisioterapia, Department of Pathology and Surgery, Miguel Hernández University, San Juan de Alicante, Alicante, Spain.

[2] Centro de Investigación Operativa, Miguel Hernández University, Elche, Alicante, Spain.

[3] Histology and Neurobiology Unit, Faculty of Medicine, Rovira i Virgili University, Reus, Spain.

* Corresponding author:

Centro de Investigación Traslacional en Fisioterapia, Department of Pathology and Surgery, Miguel Hernandez University, Crta. Alicante – Valencia, s/n, 03550, San Juan, Alicante, Spain. Email address: *clozano@umh.es*

The authors declare that all data from this study are available.

- Word count for the abstract: 192 words - Word count for the text: 5503 words

- Number of references: 35 - Number of figures: 3 - Numbers of tables: 5

Title: "**Surface and elemental analysis of stainless-steel needles after invasive physiotherapy: An exploratory scanning electron microscopy (SEM) study**"

Abstract

This study evaluated the safety and chemical variations of stainless-steel needles during human tissue application using four electrical stimulation modalities: high-intensity and low-intensity direct current, microcurrents, and compensated biphasic waves. Structural changes and surface integrity of three needle types were also analyzed via SEM. Surface analysis was performed on Type_A, Type_B, and Type_C needles (n=120) following dry needling interventions on 48 participants using four distinct electrical protocols. SEM evaluation identified carbon, oxygen, chromium, iron, nickel, silicon, manganese, and aluminum across all needles. MANOVA showed that needle type ($p < 0.001$) and electrical current ($p < 0.001$) significantly influenced surface composition. A systematic reduction in silicon occurred post-intervention ($p < 0.001$), while nickel content remained stable (6.1%–7.7%). Qualitatively, Type_A exhibited the most structural irregularities, while percutaneous electrical nerve stimulation caused the greatest organic matter accumulation. These findings indicate that invasive electrotherapy significantly alters the surface elemental composition and morphology of stainless-steel needles, notably through systematic silicon loss. While these changes indicate material loss during procedures, further tissue analysis is required to determine clinical relevance. SEM revealed that Type_A needles developed more surface scratches, whereas Type_B and Type_C accumulated substantial organic matter post-intervention.

Keywords: dry needling, dry needling needles, acupuncture needles, biocompatibility, surface degradation, stainless-steel.

Introduction

Invasive physiotherapy procedures have been used for many years to reduce pain, to increase range of motion and to improve the well-being of patients.[1–2] These therapeutic modalities involve inserting needles into pathological parts of muscles[3] and are the most commonly used techniques to treat pain caused by myofascial trigger points.[4,5] In this context, neuromodulation by percutaneous peripheral nerve stimulation with ultrasound guidance offers a different perspective regarding the use of dry needles in physical therapy.[6,7] A similar modality is high-intensity galvanic current (HIGC), which offers excellent results in the functional recovery of the tendons.[8–10] Microcurrent therapy (MC) and percutaneous electrical nerve stimulation (PENS) are other percutaneous modalities are used.[6-8,11–12]

Scanning electron microscopy (SEM) has been used in several investigations to analyze needle surface integrity. Hayhoe et al.[13] revealed that most acupuncture needles manufactured in China, Japan, and the United States showed significant manufacturing faults. In a later study, Xie et al.[14]observed irregularities or distorted points after interventions in gel pads as a simulation of human tissue. Another study evaluated the tips and the surface conditions of two types of needles of different quality and their possible alterations after performing different needling on humans.[15] Zhang et al.[16] analyzed the corrosion of stainless-steel acupuncture needles after electroacupuncture therapy in humans and found no evidence of electrolytic corrosion. Later, Margalef et al.[17] described corrosion at the tips of the needles using galvanic currents with abusive parameters, specifically defined as 50 applications of 3 mA for 3 seconds, a supra-clinical dosage that represents more than 16 times the standard clinical application of 3 repetitions. Intriago[18] used SEM to demonstrate the three-dimensional shapes and sizes of the needles and the degree of surface roughness of their polished external surfaces.

Knowledge of the therapeutic window is essential to determine the optimal energy delivery required to produce the greatest possible stimulation.[11] Aspects such as the type of current, waveform, pulse frequency, stimulation duration, current intensity, polarity, and even the needle material may be critical for treatment outcomes. The effects of these diverse applications on needle integrity have important clinical relevance. While chemical interactions with mineral or organic compounds can degrade stainless-steel, electrical stimulation can further accelerate this degradation. Electrochemical corrosion of stainless-steel can cause cytotoxicity due to the release of corrosion by products and the leaching and accumulation of metal ions in the body.[19,20] Consequently, the primary clinical aim of this study was to evaluate the safety and potential chemical variations of stainless-steel needles during their application in human tissues using four electrical stimulation modalities: high-intensity direct current (mA), low-intensity direct current (µA), square-waveform microcurrents, and compensated biphasic waves. As a secondary exploratory objective, we aimed to provide a descriptive analysis of the structural changes and surface integrity of three needle types using SEM.

Methods

Design, Setting and Participants

Prospective observational study was designed to analyze the surface composition of three different types of needles after performing different electrotherapy interventions on volunteers: in the shoulder region, HIGC or low-intensity galvanic current (LIGC), and in the leg region, PENS or MC. This study conforms to all STROBE guidelines and reports the required information accordingly (see Supplementary Checklist). The study was carried out in the physical therapy laboratory of the Center of Translational Research in Physiotherapy at the Miguel Hernández University of Elche (Alicante), and the needle analysis was carried out in the Rovira i Virgili University (Reus) in July 2021. This study was conducted within the ethical guidelines outlined in the Declaration of Helsinki and followed good clinical practice. The clinical research ethics committee of Miguel Hernández University approved the study (DPC.EPP.01.17). Each participant signed the informed consent form prior to the interventions.

Participants were recruited by advertising among students studying for the physiotherapy degree (Faculty of Medicine, Miguel Hernández University). Forty-eight university students were enrolled (24 women and 24 men). They had a mean ± standard deviation age of 24.1 ± 6.0 years and no health problems. They were randomly allocated to the shoulder group (HIGC or LIGC) or the leg group (PENS or MC). The exclusion criteria included contraindications for the techniques described: a compromised nervous system based on medical history or other conditions that increase the risk of needling; a spinal cord stimulator implant, cardiac pacemaker/defibrillator, deep brain stimulator or other implantable neurostimulator; a history of a bleeding disorder; concomitant administration of drugs (i.e. fluoroquinolones, anticoagulants, corticosteroids); or pregnancy.

Needle Characteristics and selection

Three variants of sterile, single-use stainless-steel needles of a single manufacturer (AguPunt, Spain) were analyzed. These included Type_A acupuncture needles (0.25 x 25 mm), as well as Type_B electrolysis and Type_C dry needling needles, both featuring nominal dimensions of 0.25 x 30 mm. The diameter (0.25 mm) was standardized across all groups to ensure consistent current density during electrical applications. Differences in length (25 mm vs. 30 mm) were due to manufacturer availability for specific clinical uses (acupuncture vs. dry needling).

Sample Size and Randomization

A total of 120 needles were tested (40 of each type), selected indiscriminately from different commercial batches (expiry dates: January 2024 for Type_A and Type_B; June 2023 for Type_C). All 120 needles were subjected to SEM analysis following their clinical use. Each needle was strictly linked to its assigned electrical modality to evaluate surface and chemical stability; however, individual clinical outcomes for each participant were not recorded, as the study's primary focus was the evaluation of material safety and biocompatibility. For each needle type, the 40 units were randomly assigned into five groups (n=8 per group): a control group (no intervention) and four experimental groups (MC, PENS, HIGC, and LIGC) using Microsoft Excel (see Fig. 1 and Supplementary_Needles_SEM). The sample size was calculated using G*Power 3.1.9.7, based on a multivariate analysis of variance (MANOVA) model with a significance level of 0.05, 80% power, and a medium effect size.

Ultrasound Examination

The ultrasound assessment was performed by a well-trained operator (over 10 years of experience) using a high-resolution greyscale ultrasound (GE Healthcare® Logiq R7 expert, Milwaukee, WI, USA) equipped with a 12L-RS linear probe (5–13 MHz). The procedures followed the European Society of Musculoskeletal Radiology guidelines.[21,22]

Needling Procedure and Setting

Ultrasound imaging was used to guide the placement of the needle electrode, targeting either the supraspinatus tendon (shoulder) or the quadriceps tendon (leg) within a sterile sleeve. Participants were placed in the supine position to minimise potential vagal reactions.[23] Following skin preparation with isopropyl alcohol, a guided puncture was performed at the insertional area of the quadriceps tendon, 4 cm from the superior border of the patella (Fig. 2a), or into the supraspinatus tendon (Fig. 2b). For all interventions, a single-insertion protocol was strictly followed, and the needle (25 mm or 30 mm) was inserted to its full length to ensure standardized penetration depth. To minimise mechanical confounding factors, clinicians were instructed to perform a smooth guided puncture, avoiding any aggressive thrusting or contact with the periosteum or bone.

Interventional Protocols

The needles were randomly assigned to one of the following electrical stimulation groups or a control group: for the Group 1_HIGC, a galvanic direct current was applied using a Physio Invasiva®1.0 (PRIM Physio) device, set at an intensity of 3 mA with a protocol of three pulses lasting three seconds each; for the Group 2_LIGC intervention was performed using an EPTE® Bipolar System (Ion Clinics) device, set to deliver a galvanic direct current at an intensity of 0.3 mA in a single pulse lasting 80 seconds. The placement of the neutral electrode (anode) followed the specific clinical protocols for each technology. In the case of HIGC and LIGC, patients held a hand-held neutral electrode as required by the device to close the circuit; for the Group 3_PENS, intervention was conducted using a Physio Invasiva®1.0 (PRIM Physio) device. The protocol consisted of a symmetric biphasic pulse current (100% compensated) with a 4 Hz train frequency and an 80 Hz pulse frequency. Each pulse lasted 150 μs, and the treatment was applied over 15 minutes, with the intensity adjusted to achieve minimal muscle contraction; for the Group 4_MC received microcurrent therapy via a Physio Invasiva®1.0 (PRIM Physio) device. This application involved a rectangular single-phase pulse current with an 8 Hz train frequency and a train duration ranging from 1 to 3 ms. The pulse frequency was set between 75 and 160 Hz for a 15 minutes duration, maintaining a constant intensity of 50 μA to ensure a perceptible current without inducing muscle contraction. For MC and PENS, a surface adhesive electrode was placed on the skin near the active electrode, as these systems do not utilize hand-held interfaces. This ensured that the electrical delivery for each modality adhered to standard clinical practice. Finally, Control Group: Comprised needles inserted into the target tissue following the same procedure but without the application of any electrical current.

SEM Surface Characterisation

After the interventions, scanning electron micrographs of randomly selected needles from all types (A, B, and C) were obtained to analyze chemical and morphological changes.

Chemical and Structural Analysis

A Quanta 600 SEM with an Energy Dispersive X-ray Spectroscopy (EDX) detector and X-ray microanalysis (Oxford Instruments) were used. Analysis parameters included: 20 kV voltage, 10 mm working distance, high vacuum, and 2000× magnification. No specific sample preparation was required due to the conductive nature of the needles. The analysis was performed by a technician blinded to the treatment groups (Fig. 2c and 2d).[15] Elemental composition was expressed as relative weight percentages. This approach provides a proportional distribution of the elements present on the needle surface.

Morphological and Organic Matter Assessment

A quantitative study of the morphology of the tips of the needles, the presence of organic matter on the needles and the presence of striae in the metal of the needles was also performed. Organic material is easily identifiable as rough, somewhat transparent, and sometimes intensely bright on the solid surface of the needle. Longitudinal (in the direction of the maximum length of the needle) or transverse (in the direction of the thickness of the needle) scratches can be seen on the surface of the needles. For each characteristic (tip, organic matter and scratches), the degree of involvement was quantified (Fig. 3).

Statistical Analysis

Quantitative variables are presented as the mean and standard deviation, while qualitative variables are presented as counts and percentages. Pearson linear correlation coefficients were calculated. The Central Limit Theorem allows us to assume asymptotic normality in the calculation of statistical significance (n=120). However, influential outliers were eliminated to ensure the robustness of the Pearson coefficient.

A two-way MANOVA was used to analyze the differences in the percentage of chemical elements. We used the Pillai trace for the multivariate contrasts. The effect size is included. A multivariate linear model was fitted by robust regression using a simple M estimator to eliminate potential multivariate outliers. Multiple comparisons are made using the Games-Howell test. A significance level of 0.05 was considered for all statistical analysis. R Foundation for Statistical Computing (Vienna, Austria) was used.

Results

Study Needles

One hundred and twenty AguPunt needles (40 Type_A, 40 Type_B, 40 Type_C) were evaluated with SEM (Fig. 1) (Supplementary_Needles_SEM**)**. All data generated or analysed during this study are included (Supplementary_information_files).

Primary Outcomes: Microanalysis

Table 1 shows a descriptive chemical microanalysis of the needle surfaces. The following results represent the exploratory observations of the elemental composition (mean and SD) regarding carbon, oxygen, chromium, iron, nickel, silicon, manganese and aluminium for the samples analyzed. In some needles, these elements are 0 or close to 0, so there is no value. The variations observed in the elemental composition are expressed in relative terms; therefore, a decrease in the percentage of one element may lead to a proportional increase in others, reflecting shifts in the surface chemical balance.

Type_A had the highest amount of carbon, although it decreased with longer applications. After applying any type of current, the carbon in Type_B increased. However, after percutaneous insertion, Type_A and Type_C did not show an increase in carbon after applying an electric current. At baseline, Type_A needles presented the highest percentage of surface oxygen. Following the interventions, oxygen levels decreased across all needle types; specifically, in Type_B needles, oxygen levels fell below the detection threshold.

The aluminium content was very low in the evaluated needles. Type_B showed no aluminium; it only appeared in some Type_B after PENS or MC. Type_C had the highest percentage of aluminium for all the evaluated applications.

In the samples analyzed, Type_A exhibited the least amount of silicon. In addition, after any type of application, silicon levels fell below the detection threshold in Type_A. On the other hand, silicon in Type_B or Type_C decreased significantly after the applications but did not disappear. Chromium was slightly higher in Type_B and Type_C compared with Type_A. There were no changes after applications.

Iron was the most abundant material in all of the needles. There were no significant differences in the iron percentage between the needles or applications. Similarly to iron, there were no important differences in nickel between the needles or applications, representing approximately 6% to 8% of the total elemental weight. Specifically, Type_A needles showed a baseline nickel content of 6.1% (SD 2.6), while Type_B and Type_C presented 7.7% (SD 2.3) and 7.6% (SD 0.5), respectively. Manganese was the least present in all the evaluated needles. It was completely absent in Type_A and only appeared in some needles after applying microcurrents. Overall, there were very few changes to any of the applications used or any type of needle. None of the evaluated needles presented molybdenum.

Table 2 illustrates the correlations between the analyzed chemical elements. Two primary clusters of elements with significant positive associations were identified: the first comprising carbon and oxygen ($r = 0.766$, $p < 0.001$), and the second consisting of iron, nickel, and chromium. These two clusters showed a significant negative correlation with each other, particularly between carbon and chromium ($r = -0.657$, $p < 0.001$) and iron ($r = -0.647$, $p < 0.001$). Furthermore, a third distinct behavior was observed for silicon, which presented a positive correlation with oxygen ($r = 0.478$, $p < 0.001$) and a negative correlation with iron ($r = -0.207$, $p < 0.05$). Correlation analysis revealed a strong and significant positive association between nickel, iron ($r = 0.541$, $p < 0.001$), and chromium ($r = 0.563$, $p < 0.001$).

Univariate analysis revealed that the needle factor was significant when analysing the percentage of carbon, silicon and chromium, while the electrical current factor was significant for the percentage of silicon. The needle × current interaction was significant for the percentage of carbon, silicon and iron. Based on these results, we generated a two-way MANOVA model by considering the variables carbon, silicon, iron and chromium. We included these elements because they showed a normal distribution (based on the Kolmogorov–Smirnov test) and presented significant differences in univariate analysis. We used the Pillai trace for the multivariate contrasts. We found that the needle factor ($p < 0.001$) and the current factor ($p < 0.001$) were significant, and that the needle × current interaction was almost significant ($p = 0.072$). Observations with low weights have large residual squared distances and are potential multivariate outliers with respect to the Mahalanobis fitted model. We removed these needles (4, 25, 112 and 114) (Fig. 1).

In Table 3, multivariate analysis revealed a significant needle factor for the percentage of carbon ($p = 0.043$), silicon ($p < 0.001$) and chromium ($p < 0.001$). The current factor was only significant for the percentage of silicon ($p < 0.001$). Silicon always showed significant differences after application of a current between the needles without current (WC) and the needles that had already been used for an application. We noted a significant needle × current interaction for the percentage of carbon ($p = 0.041$), silicon ($p = 0.01$) and iron ($p = 0.016$).

Multiple comparisons revealed no significant differences between Type_B and Type_C across any variables. In contrast, Type_A differed significantly from both Type_B and Type_C regarding silicon and chromium levels ($p < 0.001$). For carbon content, however, a significant difference was only observed between Type_A and Type_C ($p = 0.028$). Regarding the electrical current, silicon percentages varied significantly between the CG and all experimental groups (HIGC, LIGC, PENS, and MC), though no significant differences were found among the experimental groups themselves (Table 4).

Secondary Outcomes

From a qualitative and descriptive perspective SEM observations showed that needle tips Type_C presented a more regular and homogeneous tip morphology, followed by Type_B and finally Type_A. The tips of the needles did not noticeably deteriorate with the intervention in any of the studied models (Table 5).

When visualising needles with SEM, we usually found organic material on their surface. Organic material is easily identifiable as rough, somewhat transparent and sometimes intensely bright on the solid surface of the needle. We found organic material on all three needle types. Our qualitative analysis revealed that Type_A had less organic matter on their surface (Table 5). After insertion into human tissue, there was an increase in organic matter on all needles. PENS led to greater organic matter accumulation for all tested needles. Type_B also retain a substantial amount of organic matter after dry needling.

We sometimes observed longitudinal scratches (in the direction of the maximum length of the needle) or transverse scratches (in the direction of the thickness of the needle) on the surface of the needles. Regarding the needles prior to the intervention, longitudinal scratches were more abundant than transverse scratches on the surface of all needle types (Fig. 3; Table 5). Type_A showed the most scratches, while Type_B had the fewest scratches. However, all Type_B lost their transverse scratches after the interventions. Type_C acquired the greatest number of scratches during all of the interventions.

Discussion

The results of our surface analysis show a reduction in certain chemical elements, including metals, following the interventions. These findings support the hypothesis that such elements could potentially be retained in the participants' tissues; however, since direct tissue analysis was not performed, this remains an indirect inference that requires further confirmation. Additionally, we observed some unexpected results, such as aluminum being detected after the application of PENS or MC currents despite not being present in the control Type_B needles. This could be attributed to the unveiling of deeper layers of the alloy or complex electrochemical interactions during surface degradation. The values expressed in Table 1 are percentages; therefore, if one or more elements decrease, then the percentage of other elements with increase. For example, traces of aluminium or manganese before the interventions become detectable, although in low proportions.

In terms of carbon levels, an increase was exclusively observed on the surface of Type_B needles following the application of electric currents. In contrast, Type_A and Type_C needles did not exhibit significant variations in carbon content under the same conditions. This suggests that carbon accumulation is not a universal consequence of tissue insertion, but rather a phenomenon influenced by the specific surface characteristics or alloy composition of the Type_B needles.

Analysis of the chemical composition revealed that trace levels of aluminium were occasionally detected following the interventions (Table 1). Since aluminium is not a structural component of medical-grade stainless-steel needles, its detection is attributed to a technical artifact, likely representing background signal from the aluminium alloy needle holder used during SEM microanalysis or minor surface contamination from the manufacturing coils. These traces are toxicologically insignificant and their detection in relative percentages is often a mathematical consequence of the decrease in other surface elements, such as silicon.

In general, all needles showed a significant loss of silicon following the intervention. This outcome likely results from a combination of mechanical friction during skin and tendon penetration and the electrochemical effects of the current, which may strip the silicone-based lubricating layer or the alloy's structural silicon. While silicon is generally considered non-toxic and is even used therapeutically to counteract other toxicities, its loss leaves the metallic surface more exposed.[24]

Concurrently, our results showed variations in oxygen levels on the needle surface post-intervention. This increase in oxygenation suggests an immediate oxidation process of the stainless-steel matrix once the protective silicon layer is compromised and the needle interacts with the electrolytic environment of human tissue and the applied current. Stainless-steel is rich in chromium, and although chromium oxides can prevent surface corrosion, they do not offer complete protection under all conditions; however, much less oxidation and corrosion occurs than in ordinary steel.[25] This is a relevant factor in clinical safety, as chromium is among the most common heavy metals that cause allergies.[26] In our study, however, we did not observe significant changes in total chromium content after the interventions. This suggests that while the metal remains structurally stable, the increase in oxygen levels indicates surface chemical transformations that could facilitate the release of trace ions or alter the needle's conductivity, potentially influencing the neurophysiological response of the targeted tissue.

Toxicological thresholds and patient safety

The stability of the iron, nickel, and chromium triad across most interventions confirms their role as the structural foundation of the stainless-steel alloy used in all analyzed types of needles. This consistent metallic base, as evidenced by the strong positive correlations in Table 2, suggests that the observed changes post-intervention are primarily surface-level rather than a total structural breakdown of the needle core. The fact that these structural elements are negatively correlated with carbon and oxygen suggests that as the protective surface layer (silicon/oxygen) or organic matter (carbon) increases, the detection of the underlying metallic matrix decreases.

The detection of approximately 7% nickel across all needle types and the observed surface degradation post-intervention warrant a detailed discussion on biocompatibility. Standard surgical stainless-steel is generally considered safe; however, recent studies show that nickel release can occur from stainless-steels under certain surface conditions, particularly when the passivation layer is disrupted or during electroplating processes, potentially increasing nickel release and sensitization risk.[27]

Nickel is a potent sensitizer and, even though the exposure time in dry needling or PENS is limited, the cumulative effect of repeated treatments could potentially trigger localized hypersensitivity in susceptible patients. This finding is supported by evidence in implant and piercing literature showing that even alloys considered biocompatible may release nickel at levels relevant to allergic reactions.[28] This structural interdependence is crucial when considering that any surface degradation or 'dragging' effect during needle withdrawal could potentially expose or release these metallic ions into the host tissue. Additionally, reviews on microneedle materials highlight those metallic devices — including stainless-steel — require careful evaluation of ion release and biocompatibility, as metal ion exposure (including Ni) can contribute to localized irritation or sensitization.[29] Taking, as an example, the recent study on cosmetic microneedles by Rigali et al (2025)[30] future research could specifically analyse nickel release in acupuncture needles using the dimethylglyoxime spot test.

Furthermore, the systematic loss of silicon across all groups suggests that this coating or alloying element is being deposited in the surrounding tissue. While silicon is generally biocompatible, its displacement indicates that the needle surface is not inert under electrical stress.

These results align with previous concerns regarding metal ion migration in invasive procedures and emphasize that 'nickel-free' claims by manufacturers should be scrutinized to ensure informed consent for allergic patients.[31]

Regarding other trace elements, the manganese concentrations detected in this study (1.1%–1.7%) are in full agreement with recent assessments of surgical-grade stainless-steel (ISO 5832-1). Specifically, Pieretti et al. (2025)[32] reported manganese levels of 1.6% for this alloy, confirming that such values fall within the mandatory safety threshold of 2.0% maximum set by international standards (International Organization for Standardization - ISO 5832-1; American Society for Testing and Materials - ASTM F138). The consistency of our data with these recent findings further supports the toxicological safety of the needles tested. This safety profile is further supported by our observation that manganese levels remained relatively stable following the electrical interventions. This indicates that there was no significant net release of elements into the tissues under the conditions of this study. While chronic exposure to high manganese concentrations is known to cause manganism[33], the trace amounts identified in this study are integrated within a stable metallic matrix. Given that these concentrations fall strictly within established legal safety margins, they do not represent a toxicological risk to the patient.

The needles used in this study are said to be made of stainless surgical steel.[34] Surgical steel must contain iron, nickel, chromium and molybdenum in varying percentages. For example, the surgical steel of trans-osseous wires has the following composition: nickel 14.5%, chromium 17.6%, iron 62.5% and molybdenum 2.8%.[35] We did not detect molybdenum in the needles we evaluated.

Type_A

The needles analyzed were predominantly composed of iron and carbon, with presence of oxygen and trace amounts of silicon and manganese. Following the interventional procedures, a significant reduction in silicon was observed across all groups, while carbon levels decreased specifically during longer electrical applications. Notably, the primary metallic components—chromium, iron, manganese, and nickel—remained relatively stable. These findings suggest that the needles maintain a high degree of structural stability; however, the systematic loss of surface elements like silicon warrants further investigation to definitively rule out trace accumulation in human tissues and confirm their long-term safety profile.

Historically, Type_A have been described as having deformed and blunt tips.[13,14] However, the tips of the Type_A analyzed in the present study only showed some slight alterations. This suggests a potential improvement in manufacturing processes over recent years. Nevertheless, compared to the other types examined, Type_A tips still exhibited the highest degree of structural irregularities prior to any intervention.

Organic matter accumulation on Type_A has not been previously addressed in the literature. Our findings showed minimal biological deposits on these needles, which may be explained by their well-preserved tip morphology, reducing the likelihood of tissue dragging during insertion and withdrawal. This contrasts with Xie et al.[14] who observed that deformed tips were more prone to capturing material from the insertion site. However, after PENS application, Type_A needles exhibited a moderate accumulation of organic matter. This suggests that electrochemical polarity—rather than mechanical trauma—could be the primary factor driving the attraction of biological residues, a pattern consistent with the other needle types analyzed in this study.

Type_A showed the greatest number of longitudinal and transverse scratches, perhaps because they are made of lower-quality steel, which would also explain why the tips are more deformed. The transverse scratches possibly come from the metal coils (wire drawing process) used during manufacturing. However, longitudinal scratches are more likely to come from manufacturing when they are introduced into the tubes in which they are sold. Insertion into tissue polishes the scratches, especially the transverse ones. It is then possible that steel shavings accumulate in tissues. Xie et al.[14] took scanning electron micrographs of Type_A after standard manipulation in needling practice gel. These authors detected metallic remains of the Type_A in the gel. They also observed the existence of striations or scratches but did not describe whether they were modified by the insertion into the gel.

Type_B

These needles were especially rich in iron and poor in oxygen and silicon. After the procedures, the silicon of the Type_B decreased markedly; the oxygen levels fell below the detection threshold; and the chromium, iron, manganese and nickel changed very little. These needles are made of high-quality steel. Margalef et al.[17] described that electric current do not produce loss of metals or modification of the morphology of Type_B. However, if abusive parameters are employed, alterations to the needle may occur. It is important to note that these parameters (e.g., 50 applications) represent a supra-maximal experimental dosage used to test safety limits; such conditions are not reached in clinical practice, where typically only 3 applications are performed. Therefore, the structural integrity of the needle is maintained within the therapeutic range.

These needles carried a lot of organic matter after the application of any form of electricity. Because the tips are practically not altered by tissue insertion, the organic matter possibly accumulates due to electrostatic attraction.

Similarly to Type_A, the transverse scratches disappeared completely after any intervention, probably due to transdermal insertion. We also assume that steel shavings remain in the tissues after the interventions. There was an increase in longitudinal scratches after all interventions. As in previous cases, we assume that it is due to transdermal insertion or repositioning in the guide tube.

Type_C

These needles were especially rich in nickel and chromium iron, which corresponds to a surgical steel alloy. For this reason, the tips of these needles are difficult to deform. Similarly to Type_B, the organic matter carried by Type_C after the application of any form of electricity is possibly from electrostatic attraction. These needles also had fewer scratches, but after any intervention the number of scratches increased. Because the stretches were not polished, it is unlikely that metal chips accumulate in tissues. Overall, Type_C seem to be the best made.

The identification of these surface irregularities and elemental changes suggests potential implications for clinical safety. Any alteration in needle integrity - such as tip deformation or the polishing of manufacturing scratches - could theoretically influence the distribution of current density at the tip or might lead to the deposition of metallic micro-residues in the tissue. These observations underscore the importance of considering material stability when evaluating the biocompatibility of invasive electrical interventions.

Limitations of the study

A primary limitation of this study is the evaluation of a single needle brand (AguPunt). While this brand is one of the frequently used within the Spanish clinical context for invasive physiotherapy, manufacturing processes, surface treatments, and specific alloy compositions (including the thickness of the silicone coating) can vary significantly between manufacturers. Therefore, the observed patterns of elemental loss and surface degradation may not be directly generalizable to other brands available in different international markets. Additionally, the assessment of organic matter was purely qualitative, based on visual SEM observation. This limits the objective quantification of the volume and exact nature of biological deposits. Future research should employ quantitative approaches, such as digital image processing for area measurement or proteomic analysis of the needle surface, to more precisely determine the amount and composition of the organic residue retained after each intervention.

Moreover, all interventional procedures were performed by a single experienced physiotherapist. While this approach ensured high intra-operator reliability and standardized the needle handling across all experimental groups, it may limit the generalizability of the findings to different clinical handling styles or varying levels of expertise. Furthermore, a limitation of the study is the slight variation in needle length between groups (25 mm for Type_A vs. 30 mm for Type_B and Type_C) due to manufacturer availability. Although we standardized the needle diameter to 0.25 mm across all groups to maintain consistent current density and mechanical properties, future studies using identical lengths for all needle types would further strengthen the generalizability of these findings.

Concerning the chemical characterization, the analysis conducted via EDX provides relative elemental percentages rather than absolute quantification. This characterization means that a significant decrease in one element (such as Silicon) may result in a proportional apparent increase in the relative percentages of other surface elements. This inherent property of the analytical method should be considered when interpreting the compositional shifts observed across the different needle types.

Despite the rigor of the SEM analysis, the relationship between the observed needle surface damage and patient symptoms or adverse events was not empirically tested; thus, our findings are exploratory and focus on material integrity rather than direct clinical outcomes. Additionally, while we standardized the procedures, the study design does not allow for a fully isolated comparison of all individual factors in a controlled laboratory environment. Consequently, any suggestion that needle surface condition may influence current density or biocompatibility should be treated as a hypothesis to be tested in future clinical research.

Finally, a significant limitation of this study is that we did not measure the actual transfer of metallic elements or microscopic debris into the participants' tissues, nor did we evaluate the potential clinical consequences of the observed needle degradation. Our findings are strictly limited to the physical and compositional changes of the needle itself. Future clinical and histological studies are required to determine whether these microscopic variations have any biological impact or long-term clinical effects on the patient.

Conclusions

In summary, our study demonstrates that invasive electrotherapy procedures lead to significant changes in the surface elemental composition and morphology of stainless-steel needles. Specifically, we observed a systematic loss of silicon across all needle types and variations in carbon levels after the application of electric currents. While these surface alterations suggest the potential for elemental deposition within human tissues, this remains a hypothesis that requires direct confirmation through tissue analysis. Furthermore, SEM analysis revealed that Type_A needles exhibited the highest number of surface scratches, while Type_B and Type_C needles showed substantial accumulation of organic matter. These findings highlight the importance of considering needle degradation as a factor in the interaction between the needle and the biological medium. Future research should prioritize quantifying the exact amount of elemental deposition (such as Si, Ni, or Cr) in human tissues using histological analysis or mass spectrometry.

Conflict of interest

None of the authors has a financial or other interest relating to this manuscript.

Funding Declaration

José V. Segura acknowledges the financial support received from the Chair of Economic Model Transformation at the Department of Economy, Finance and Public Administration (Conselleria d'Economia, Hisenda i Administració Pública) of the Valencian Government. The remaining authors declare that no specific funding was received for this study from any public, commercial, or not-for-profit sectors.

Author contribution statement

Carlos Lozano-Quijada, Emilio Poveda-Pagán, José Vicente Toledo Marhuenda and Manel Santafé conceived and designed the experiments. Manel Santafé, Carlos Lozano-Quijada and Emilio Poveda-Pagán performed the needle analysis with SEM. Carlos Lozano-Quijada, Emilio Poveda-Pagán, Manel Santafé and José Vicente Toledo Marhuenda wrote the manuscript and prepared the figures. José Vicente Segura-Heras performed the statistical analysis.

Data availability

All data generated or analysed during this study are included in this published article [and its supplementary information files].

References

1. Berger AA, Liu Y, Mosel L, Champagne KA, et al. Efficacy of Dry Needling and Acupuncture in the Treatment of Neck Pain. Anesth Pain Med. 2021 Apr 3;11(2):e113627. https://doi.org/10.5812/aapm.113627.

2. Valera-Calero JA, Fernández-de-Las-Peñas C, Navarro-Santana MJ, Plaza-Manzano G. Efficacy of Dry Needling and Acupuncture in Patients with Fibromyalgia: A Systematic Review and Meta-Analysis. Int J Environ Res Public Health. 2022 Aug 11;19(16):9904. https://doi.org/10.3390/ijerph19169904.
3. Dommerholt J. Dry needling - peripheral and central considerations. J Man Manip Ther. 2011 Nov;19(4):223-7. https://doi.org/10.1179/106698111X13129729552065.
4. Benito-de-Pedro AI, Becerro-de-Bengoa-Vallejo R, Losa-Iglesias ME, Rodríguez-Sanz D, Calvo-Lobo C, Benito-de-Pedro M. Efficacy of Deep Dry Needling versus Percutaneous Electrolysis in Ultrasound-Guided Treatment of Active Myofascial Trigger Points of the Levator Scapulae in Short-Term: A Randomized Controlled Trial. Life (Basel). 2023 Apr 3;13(4):939. https://doi.org/10.3390/life13040939.
5. Gerwin RD. A New Unified Theory of Trigger Point Formation: Failure of Pre- and Post-Synaptic Feedback Control Mechanisms. Int J Mol Sci. 2023 May 2;24(9):8142. https://doi.org/10.3390/ijms24098142.
6. Beltran-Alacreu H, Serrano-Muñoz D, Martín-Caro Álvarez D, Fernández-Pérez JJ, Gómez-Soriano J, Avendaño-Coy J. Percutaneous Versus Transcutaneous Electrical Nerve Stimulation for the Treatment of Musculoskeletal Pain. A Systematic Review and Meta-Analysis. Pain Med. 2022 Aug 1;23(8):1387-1400. https://doi.org/10.1093/pm/pnac027.
7. lfeld BM, Plunkett A, Vijjeswarapu AM, et al. Percutaneous Peripheral Nerve Stimulation (Neuromodulation) for Postoperative Pain: A Randomized, Sham-controlled Pilot Study. Anesthesiology. 2021 Jul 1;135(1):95-110. https://doi.org/10.1097/ALN.0000000000003776.

8. Abat F, Gelber PE, Polidori F, Monllau JC, Sanchez-Ibañez JM. Clinical results after ultrasound-guided intratissue percutaneous electrolysis (EPI®) and eccentric exercise in the treatment of patellar tendinopathy. Knee Surg Sports Traumatol Arthrosc. 2015 Apr;23(4):1046-52. https://doi.org/10.1007/s00167-014-2855-2.
9. Asensio-Olea L, Leirós-Rodríguez R, Marqués-Sánchez MP, de Carvalho FO, Maciel LYS. Efficacy of percutaneous electrolysis for the treatment of tendinopathies: A systematic review and meta-analysis. Clin Rehabil. 2023 Jun;37(6):747-759. https://doi.org/10.1177/02692155221144272.
10. Augustyn D, Paez A. The effectiveness of intratissue percutaneous electrolysis for the treatment of tendinopathy: a systematic review. S Afr J Sports Med. 2022 Jan 1;34(1):v34i1a12754. https://doi.org/10.17159/2078-516X/2022/v34i1a12754.
11. Poltawski L, Johnson M, Watson T. Microcurrent therapy in the management of chronic tennis elbow: pilot studies to optimize parameters. Physiother Res Int. 2012 Sep;17(3):157-66. https://doi.org/10.1002/pri.526.
12. Sánchez-Infante J, Navarro-Santana MJ, Bravo-Sánchez A, Jiménez-Diaz F, Abián-Vicén J. Is Dry Needling Applied by Physical Therapists Effective for Pain in Musculoskeletal Conditions? A Systematic Review and Meta-Analysis. Phys Ther. 2021 Mar 3;101(3):pzab070. https://doi.org/10.1093/ptj/pzab070.
13. Hayhoe S, McCrossan M, Smith A, Ellis D, Croft S, Mei MF. Single-use acupuncture needles: scanning electron-microscopy of needle-tips. Acupunct Med. 2002 Mar;20(1):11-8. https://doi.org/10.1136/aim.20.1.11.
14. Xie YM, Xu S, Zhang CS, Xue CC. Examination of surface conditions and other physical properties of commonly used stainless steel acupuncture needles.

Acupunct Med. 2014 Apr;32(2):146-54. https://doi.org/10.1136/acupmed-2013-010472.

15. Poveda-Pagán EJ, Hernández-Sánchez S, Rhys-Jones-López L, Palazón-Bru A, Lozano-Quijada C. Scanning electron microscopy examination of needle tips after different procedures of deep dry needling in humans. Sci Rep. 2018 Dec 19;8(1):17966. https://doi.org/10.1038/s41598-018-36417-w.

16. Zhang CS, Zhang GS, Xu S, Li B, Zhang AL, Xue CC, Xie YM. Examination of needle surface corrosion in electroacupuncture. Acupunct Med. 2018 Dec;36(6):367-376. https://doi.org/10.1136/acupmed-2017-011542.

17. Margalef R, Bosque M, Minaya-Muñoz F, Valera-Garrido F, Santafe MM. Safety analysis of percutaneous needle electrolysis: a study of needle composition, morphology, and electrical resistance. Acupunct Med. 2021 Oct;39(5):471-477. https://doi.org/10.1177/0964528420988007.

18. Intriago V, Reina MA, Boezaart AP, Tubbs RS, Montaña AV, Pérez-Rodríguez FJ, Sanroman-Junquera M. Microscopy of structures surrounding typical acupoints used in clinical practice and electron microscopic evaluation of acupuncture needles. Clin Anat. 2022 Apr;35(3):392-403. https://doi.org/10.1002/ca.23845.

19. Es-Souni M, Es-Souni M, Fischer-Brandies H. Assessing the biocompatibility of NiTi shape memory alloys used for medical applications. Anal Bioanal Chem. 2005 Feb;381(3):557-67. https://doi.org/10.1007/s00216-004-2888-3.

20. Roodenburg B, Morren J, Berg HE, de Haan SWH: Metal release in a stainless steel pulsed electric field (PEF) system: part I Effect of different pulse shapes; theory and experimental method Innov Food Sci Eng Technol 2005, 6(3):327–336. https://doi.org/10.1016/j.ifset.2005.04.004

21. Beggs I, Bianchi S, Bueno A, et al. (2020). European society of MusculoSkeletal radiology. Ultrasound group protocols. musculoskeletal ultrasound technical guidelines: I. shoulder. https://www.essr.org/subcommittees/ultrasound/.

22. Beggs I, Bianchi S, Bueno A, et al. (2020). European society of MusculoSkeletal radiology. Ultrasound group protocols. musculoskeletal ultrasound technical guidelines: V. knee. https://www.essr.org/subcommittees/ultrasound/.

23. de la Cruz Torres B, Albornoz Cabello M, García Bermejo P, Naranjo Orellana J. Autonomic responses to ultrasound-guided percutaneous needle electrolysis of the patellar tendon in healthy male footballers. Acupunct Med. 2016 Aug;34(4):275-9. https://doi:10.1136/acupmed-2015-010993.

24. Okeke ES, Nweze EJ, Ezike TC, Nwuche CO, Ezeorba TPC, Nwankwo CEI. Silicon-based nanoparticles for mitigating the effect of potentially toxic elements and plant stress in agroecosystems: A sustainable pathway towards food security. Sci Total Environ. 2023 Jul 17;898:165446. https://doi.org/10.1016/j.scitotenv.2023.165446.

25. Lo KH, Shek CH, Lai JKL. Recent developments in stainless steels. Mater Sci Eng R Rep. 2009;65(4–6):39–104. https://doi.org/10.1016/j.mser.2009.03.001

26. Chamani S, Mobasheri L, Rostami Z, Zare I, Naghizadeh A, Mostafavi E. Heavy metals in contact dermatitis: A review. J Trace Elem Med Biol. 2023 Sep;79:127240. https://doi.org/10.1016/j.jtemb.2023.127240.

27. Emanuele R, Comparini A, Verrucchi M, Del Pace I, Meoli A, Vorobyova M, Giurlani W, Innocenti M. Nickel Release From 316L Stainless Steel Following A Ni-Free Electroplating Cycle. Heliyon. 2024 Aug 29;10(17):E37125. https://doi.org/10.1016/J.Heliyon.2024.E37125.

28. Von Spreckelsen B, Jensen MB, Johansen JD, Ahlström MG. Nickel Allergy And Piercings: A Systematic Review And Meta-Analysis. Contact Dermatitis. 2025 Oct;93(4):275-284. https://doi.org/10.1111/Cod.14837.

29. Aldawood FK, Andar A, Desai S. A Comprehensive Review Of Microneedles: Types, Materials, Processes, Characterizations And Applications. Polymers (Basel). 2021 Aug 22;13(16):2815. https://doi.org/10.3390/polym13162815.
30. Rigali S, Zeng C, Scheman A, Moraga R, Liszewski W. Nickel Secretion And The Allergenic Potential Of Cosmetic Microneedles. Dermatol Surg. 2025 Oct 13. https://doi.org/10.1097/DSS.0000000000004910.
31. Reclaru L, Grecu AF, Grecu DF, Lungulescu CV, Grecu DC. Corrosion and Ion Release in 304L Stainless Steel Biomedical Stylets. Materials (Basel). 2025 Aug 11;18(16):3769. https://doi.org/10.3390/ma18163769.
32. Pieretti EF, Piaggio D, Costa I. Assessment of the Surface Characteristics of ISO 5832-1 Stainless Steel for Biomaterial Applications. Materials (Basel). 2025 Aug 27;18(17):4020. doi: 10.3390/ma18174020.
33. Dorman DC. The Role of Oxidative Stress in Manganese Neurotoxicity: A Literature Review Focused on Contributions Made by Professor Michael Aschner. Biomolecules. 2023 Jul 28;13(8):1176. https://doi.org/10.3390/biom13081176.
34. AguPunt website, https://agupunt.com/?lang=en [accessed 13 February 2026].
35. Nwashindi A, Dim EM. Adverse effects of nickel in transosseous wires and surgical implants: literature review. Niger J Med. 2014 Oct-Dec;23(4):335-43.

Figure legends

Fig. 1. Flow diagram of needles. Type_A, acupuncture needles; Type_B, electrolysis needles; Type_C, dry needling needles; HIGC, high-intensity galvanic current therapy; LIGC, low-intensity galvanic current therapy; PENS, percutaneous electrical nerve stimulation therapy; MC, microcurrent therapy.

Fig. 2. Needle location in the different interventions and scanning electronic microscopy. (a) Location of the needle in the lower limb for microcurrent (MC) therapy and percutaneous electrical nerve stimulation (PENS); the needle was located with ultrasound. (b) Example of how to apply galvanic currents to the supraspinatus

tendon; the needle was located with ultrasound. (c1) Scanning electronic microscope and sample holder. (c2) Example of a needles in the sample holder.

Fig. 3. Examples of the needle tip, organic matter and scratches on the surface of the needles. Each characteristic was classified according to intensity: grade 0, absent; grade 1, mild; grade 2, moderate; grade 3, intense. **Note:** No examples of grade 3 are shown as this intensity was not observed in any of the analyzed samples.

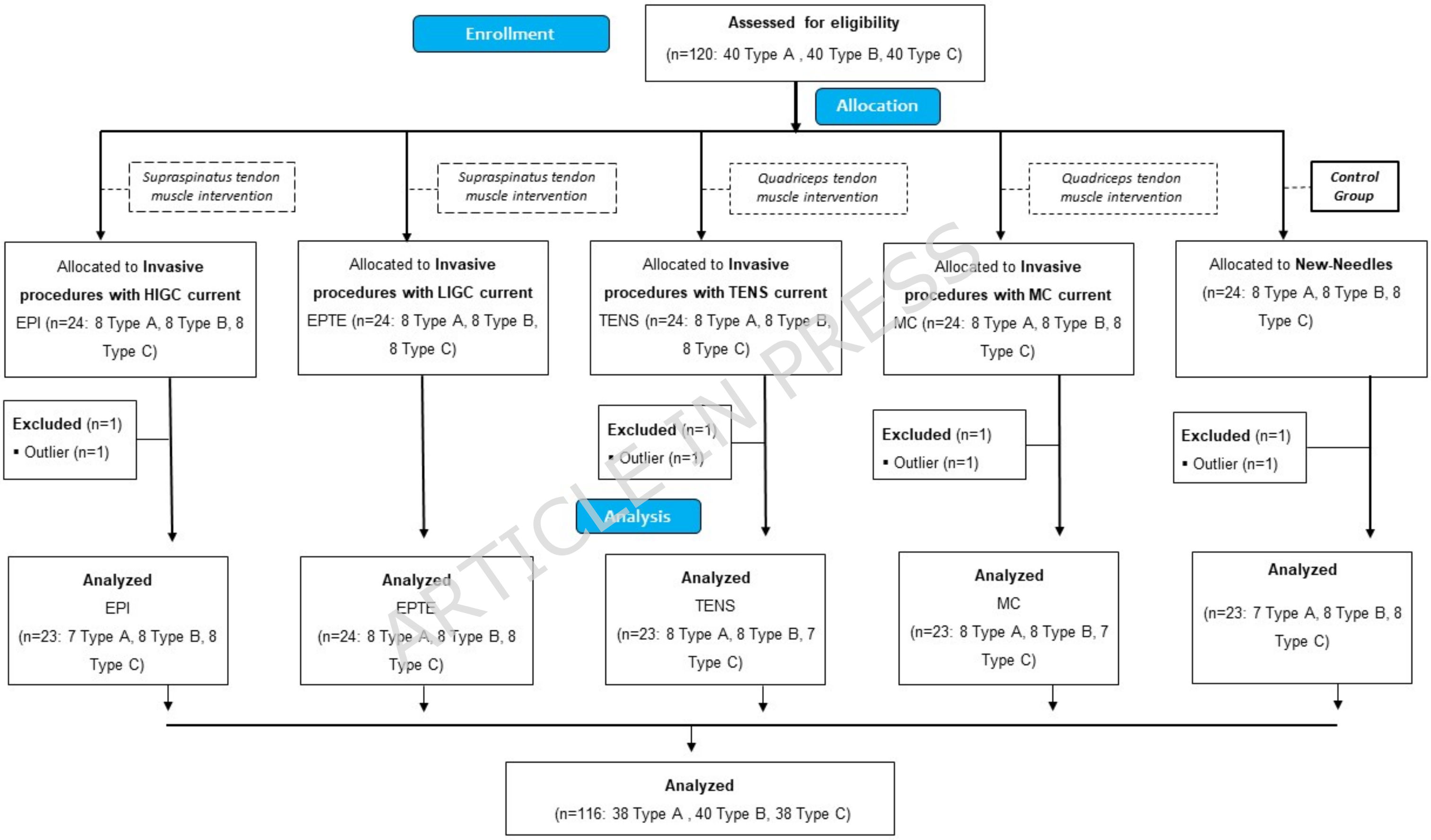
Enrollment
Assessed for eligibility
(n=120: 40 Type A , 40 Type B, 40 Type C)
Allocation
Supraspinatus tendon muscle intervention
Supraspinatus tendon muscle intervention
Quadriceps tendon muscle intervention
Quadriceps tendon muscle intervention
Control Group
Allocated to Invasive procedures with HIGC current EPI (n=24: 8 Type A, 8 Type B, 8 Type C)
Allocated to Invasive procedures with LIGC current EPTE (n=24: 8 Type A, 8 Type B, 8 Type C)
Allocated to Invasive procedures with TENS current TENS (n=24: 8 Type A, 8 Type B, 8 Type C)
Allocated to Invasive procedures with MC current MC (n=24: 8 Type A, 8 Type B, 8 Type C)
Allocated to New-Needles (n=24: 8 Type A, 8 Type B, 8 Type C)
Excluded (n=1) ▪ Outlier (n=1)
Excluded (n=1) ▪ Outlier (n=1)
Excluded (n=1) ▪ Outlier (n=1)
Excluded (n=1) ▪ Outlier (n=1)
Analysis
Analyzed EPI (n=23: 7 Type A, 8 Type B, 8 Type C)
Analyzed EPTE (n=24: 8 Type A, 8 Type B, 8 Type C)
Analyzed TENS (n=23: 8 Type A, 8 Type B, 7 Type C)
Analyzed MC (n=23: 8 Type A, 8 Type B, 7 Type C)
Analyzed (n=23: 7 Type A, 8 Type B, 8 Type C)
Analyzed (n=116: 38 Type A , 40 Type B, 38 Type C)

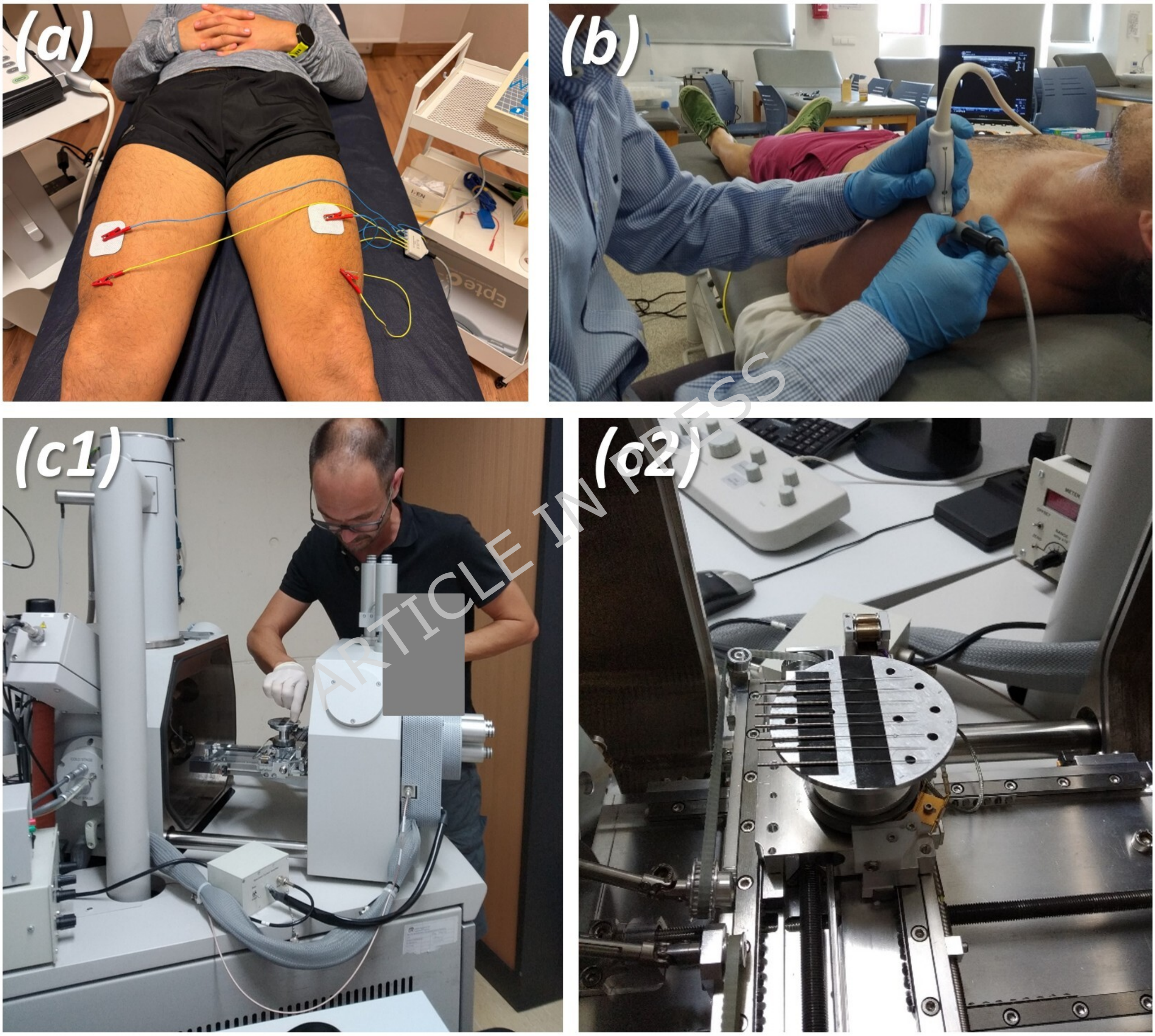
(a)
(b)
(c1)
(c2)

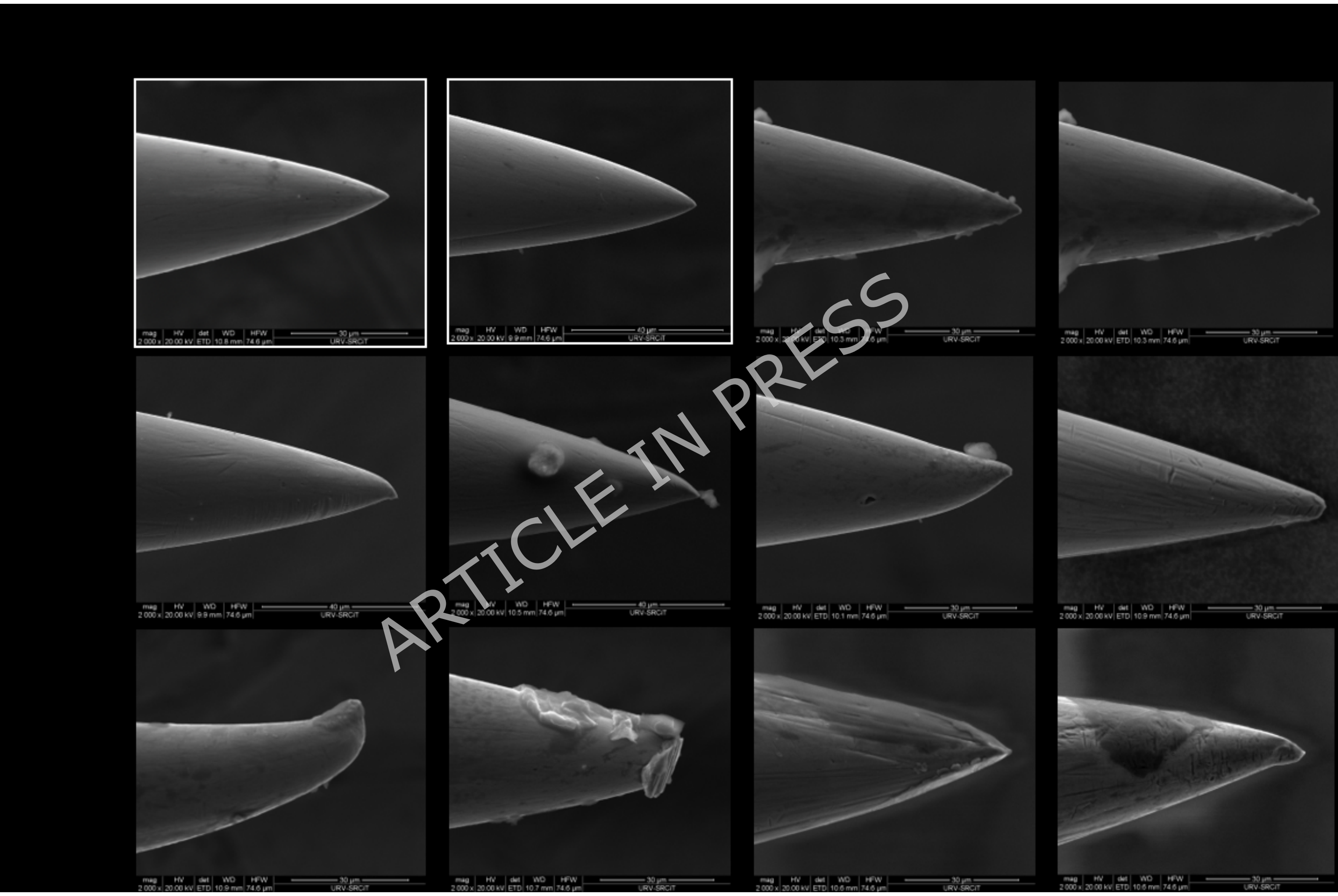

TABLE 1. Descriptive chemical elements for needle and current.

Element	Needle	CG mean (SD)	HIGC mean (SD)	LIGC mean (SD)	PENS mean (SD)	MC mean (SD)
Carbon	Type_A	12.6 (19.8)	11.9 (17.8)	5.7 (4.3)	3.6 (4.7)	5.1 (2.9)
	Type_B	1.6 (3)	2.2 (1.4)	4.2 (3.7)	7 (5.8)	4.5 (1.1)
	Type_C	4.7 (3.2)	3.2 (1.7)	2.8 (2)	2.3 (2.5)	4.2 (5.4)
Oxygen	Type_A	1 (2.8)	1.1 (3.2)	0.3 (0.9)	0.2 (0.5)	0.3 (0.9)
	Type_B	0.2 (0.6)	0 (0)	0 (0)	0 (0)	0 (0)
	Type_C	0.7 (1.2)	0 (0)	0.2 (0.6)	0 (0)	1.3 (2.9)
Aluminum	Type_A	0 (0)	0.1 (0.3)	0.3 (0.7)	0 (0)	0.5 (0.5)
	Type_B	0 (0)	0 (0)	0 (0)	0.1 (0.2)	0.3 (0.4)
	Type_C	0.2 (0.4)	0.3 (0.5)	0.3 (0.9)	0.4 (0.7)	0.1 (0.3)
Silicon	Type_A	0.6 (0.5)	0 (0)	0 (0)	0 (0)	0 (0)
	Type_B	0.9 (0.5)	0.3 (0.5)	0.2 (0.4)	0.8 (0.3)	0.7 (0.4)
	Type_C	1.8 (0.9)	0.5 (0.4)	0.5 (0.4)	0.5 (0.5)	1.6 (3.4)
Chromium	Type_A	17 (4.4)	16.9 (4.1)	18.3 (1.2)	18.8 (1.1)	18.7 (0.6)
	Type_B	20.6 (0.7)	20.4 (0.4)	20.3 (1)	19.5 (1.1)	19.9 (0.3)
	Type_C	19.4 (0.9)	20.2 (0.5)	20.2 (0.7)	17.8 (7.2)	19.4 (2.4)
Iron	Type_A	62.7 (16.3)	63 (14.6)	67.1 (4.8)	70.2 (3.1)	67.7 (2.1)
	Type_B	68.6 (2.7)	69.4 (2.9)	67.6 (2.4)	65.4 (4.3)	66.6 (0.7)
	Type_C	65.4 (3.5)	67.5 (1.6)	68.4 (0.9)	60.6 (24.6)	65.5 (8.3)
Nickel	Type_A	6.1 (2.6)	7 (3.4)	8.3 (1.1)	7.2 (1.5)	7.5 (1.4)
	Type_B	7.7 (2.3)	7.3 (1.8)	7.7 (0.6)	7 (0.5)	7.6 (0.3)
	Type_C	7.6 (0.5)	7.8 (0.6)	7.4 (0.7)	6 (3)	7.7 (1.1)
Manganese	Type_A	0 (0)	0 (0)	0 (0)	0 (0)	0.2 (0.4)
	Type_B	0.4 (0.8)	0.4 (0.8)	0 (0)	0.2 (0.6)	0.4 (0.7)
	Type_C	0.2 (0.5)	0.5 (0.8)	0.2 (0.5)	0 (0)	0.2 (0.4)

CG (Control Group) HIGC (High-Intensity Galvanic Current), LIGC (Low-Intensity Galvanic Current), PENS (Percutaneous Electrical Nerve Stimulation), MC (Micro-Current Therapy), Type_A (Acupuncture needles), Type_B (Electrolysis needles), Type_C (Dry needles).

TABLE 2. The correlation of the different elements analyzed.

	Carbon	Oxygen	Aluminum	Silicon	Chromium	Iron	Nickel	Manganese
Carbon	1	0	0.777	0.242	0	0	0	0.22
Oxygen	0.766**	1	0.97	0	0	0	0	0.786
Aluminum	-0.026	0.003	1	0.496	0.916	0.901	0.915	0.728
Silicon	0.108	0.478**	-0.063	1	0.373	0.023	0.45	0.095
Chromium	-0.657**	-0.573**	0.01	-0.082	1	0	0	0.586
Iron	-0.647**	-0.611**	0.011	-0.207*	0.926**	1	0	0.894
Nickel	-0.497**	-0.411**	0.01	-0.07	0.563**	0.541**	1	0.163
Manganese	-0.113	0.025	0.032	0.153	0.05	0.012	0.128	1

Correlation coef.; * p<0.05; ** p<0.001 Diagonal lower present Pearson correlation coef. and upper diagonal p-values

TABLE 3. Multivariate one-way ANOVA model fitted for each chemical element (p-value).

		Df	Sum Sq	Mean Sq	F value	p-value	eta.sq
Carbon	Needle	2	71.20	35.60	3.24	0.043	0.050
	Current	4	7.61	1.90	0.17	0.952	0.006
	Needle:Current	8	185.92	23.24	2.11	0.041	0.135
	Residuals	101	1111.09	11.00			
Silicon	Needle	2	9.08	4.54	22.70	0.000	0.191
	Current	4	11.79	2.95	14.73	0.000	0.260
	Needle:Current	8	4.32	0.54	2.70	0.010	0.095
	Residuals	101	20.20	0.20			
Chromium	Needle	2	61.86	30.93	42.87	0.000	0.422
	Current	4	0.32	0.08	0.11	0.978	0.002
	Needle:Current	8	11.13	1.39	1.93	0.064	0.076
	Residuals	101	72.87	0.72			
Iron	Needle	2	12.83	6.41	0.75	0.474	0.012
	Current	4	16.27	4.07	0.48	0.752	0.015
	Needle:Current	8	171.18	21.40	2.51	0.016	0.161
	Residuals	101	860.69	8.52			

Df (degrees freedom), Sum Sq (sum of squares), Mean Sq (mean squares), eta sq (effect size).

TABLE 4. Multiple comparisons within each significant factor (Games-Howell test).

	Variable	Group1	Group2	p-values	p.adj.signif
Needle	**Carbon**	Type A	Type B	0.31	Ns
		Type A	Type C	**0.028**	*
		Type B	Type C	0.638	Ns
	Silicon	Type A	Type B	**0**	****
		Type A	Type C	**0**	****
		Type B	Type C	0.37	Ns
	Chromium	Type A	Type B	**0**	****
		Type A	Type C	**0**	****
		Type B	Type C	0.856	Ns
Current	**Silicon**	CG	HIGC	**0.002**	**
		CG	LIGC	**0.001**	***
		CG	TENS	**0.014**	*
		CG	MC	**0.007**	**

CG (Control Group) HIGC (High-Intensity Galvanic Current), LIGC (Low-Intensity Galvanic Current), PENS (Percutaneous Electrical Nerve Stimulation), MC (Micro-Current Therapy), Type_A (Acupuncture needles), Type_B (Electrolysis needles), Type_C (Dry needles).

TABLE 5. Morphological analysis.

		Needle tip		Organic material		Striae Long.		Striae Trans.	
Needle	**Procedure**	Mean	SD	Mean	SD	Mean	SD	Mean	SD
Type_A	Before	1.06	0.77	0.75	0.65	1.25	0.38	1.25	0.46
	HIGC	0.87	0.58	0.93	0.73	1.37	0.52	0.75	0.70
	LIGC	0.81	0.65	0.56	0.68	1.37	0.52	0.81	0.65
	PENS	0.57	0.78	1.18	0.70	0.37	0.52	0.44	0.68
	MC	0.31	0.45	0.93	0.56	0.50	0.46	0.19	0.37
Type_B	Before	0.86	0.48	0.86	0.75	0.43	0.53	0.14	0.38
	HIGC	0.56	0.56	0.88	0.64	0.88	0.23	0.00	0.00
	LIGC	0.5	0.58	1.19	0.37	0.75	0.27	0.00	0.00
	PENS	0.13	0.23	1.31	0.65	0.81	0.46	0.00	0.00
	MC	0.43	0.61	1.31	0.59	1.06	0.42	0.00	0.00
Type_C	Before	0.19	0.37	1.19	0.37	0.88	0.35	0.06	0.18
	HIGC	0.06	0.18	1.44	0.50	1.06	0.42	0.31	0.53
	LIGC	0.13	0.35	0.69	0.70	1.06	0.32	0.19	0.53
	PENS	0.17	0.41	1.50	0.50	1.57	0.45	0.07	0.19
	MC	0.00	0.00	0.94	0.82	1.00	0.32	0.29	0.27

Before, needles just removed from the package before performing any procedure. The degree of involvement has been quantified as: 0, absent; 1, slight; 2 moderate; 3, serious. No needle has reached grade 3. An average of the values obtained in each needle and procedure has been performed. Values close to 0 indicate little affectation and values close to 2 indicate greater affectation. HIGC (High-Intensity Galvanic Current), LIGC (Low-Intensity Galvanic Current), PENS (Percutaneous Electrical Nerve Stimulation), MC (Micro-Current Therapy).